The tidal channel morphodynamics in the Yangtze Estuary: a case of the South Branch

Leicheng Guo [1,2], Mick van der Wegen [1,3], Dano Roelvink [1,3], Qing He [2]

Abstract

The South Branch (SB) in the Yangtze Estuary (YE) is a fluvial dominated channel. Its morphology is characterized by large scaled meanders in the presence of both mid-channel and bank-attached sands. Historical bathymetrical analysis shows that the morphodynamic evolution is largely influenced by human activities in reclaiming the sands and protecting the coastlines before 1958. After that, the SB is accreted on the shoal and eroded in the channel, developing toward a matured channel-shoal pattern with associated downward and lateral sand movements and channel migration.

We apply long-term morphodynamic model to examine the evolution of SB and its governing mechanisms. The model hindcasts the historical evolution for 50 years and produces the channel pattern fairly well. Sensitivity analysis indicates that the river discharge also plays an essential role by supplying sediment and flushing sediment downward. The geometry is important in controlling the location and scale of the meanders. The overtide is fundamental in stimulating sediment deposition by generating a flood tidal asymmetry.

Key words: Morphodynamic, Yangtze Estuary, Fluvial channel

1. Introduction

The YE is a large fluvial estuary developed based on a giant Holocene delta. Benefiting from huge riverine sediment input, the Holocene incised Yangtze valley is filled and the Yangtze delta is built up both sub-aerially and sub-aqueously. The modern YE then developed over the delta with channels and bars formed.

The YE morphodynamics are mainly driven by river discharge, macro-tide and moderate wave conditions. The river discharge varies in a seasonal cycle from 10,000 m^3/s in the dry seasons to 50,000 m^3/s in the wet seasons. During extremely large flood period, the discharge is up to 90,000 m^3/s. The river discharge plays a significant role in controlling the saltwater intrusion, water residence time and morphodynamics in YE (Wu et al., 2010; Wang et al., 2010; Yun, 2004). The Yangtze River supplies about 414 million tons sediment to the estuary per year, in which most of them are fine materials. Approximately half of the river-born sediment deposits in the estuary whereas the other half is transported offshore.

The mean tidal range in mouth zone of YE is about 2.6 m while the spring tide range is up to 4.5 m. The tidal current is circulating in the nearshore while it is reversing inside the estuary. The wave climate in YE is characterized by a mean wave height of 0.9 m in the mouth zone which is thought to be secondary forcing except the episodic summer typhoons. In all the YE is a fluvial and tidal dominated system.

Morphologically, the present YE can be subdivided into three zones: the tide-dominated North Branch (NB), the fluvial dominated South Branch (SB) and the mouth zone (MZ) (Fig 1). The NB receives little river discharge nowadays due to its degenerated inlet conditions and funnel shaped geometry. The SB is the major channel conveying riverine water and sediment seaward. The mouth zone covers the turbidity maximum and is open to the sea and is characterized by extensive sands and shallow channels.

[1] UNESCO-IHE, PO Box 3015, Delft 2601DA, the Netherlands, l.guo@unesco-ihe.org
[2] Estuarine and Coastal Institute, East China Normal Univeristy, Shanghai, China
[3] Deltares, PO Box 177, Delft 2600MH, the Netherlands, d.roelvink@unesco-ihe.org

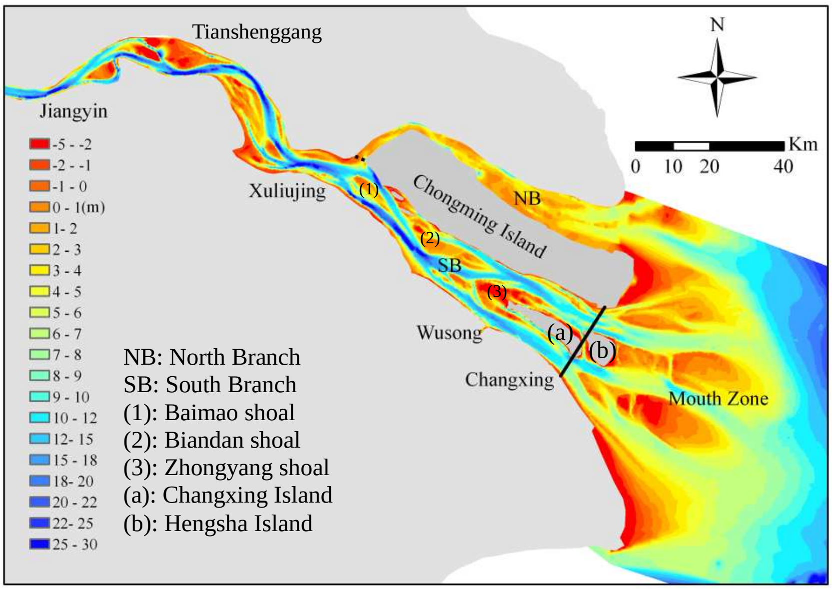

Fig 1 The geometry and bathymetry of YE in 1997

With excessive riverine sediment input, the YE has experienced deposition and accretion over the past centuries. Also it is subject to extensive human activities in terms of diking, reclamation, channel training etc (Yun, 2004). Literature survey shows that a number of field studies and hydrodynamic modelling efforts on the YE has been paid, but less on its morphodynamics (Yun, 2004; Hu et al. 2009). Generally, schematized morphodynamic modelling studies concentrate on tide- or wave-dominated basins, where river discharge is minor or negligible (Hibma et al., 2004; van der Wegen and Roelvink, 2012 etc). Therefore we take the SB in YE as an example of fluvial channel to investigate its morphodynamic evolution and the governing mechanisms.

The SB, locates inside the YE, is dominated both river and tidal forcing. The mean tidal range is about 2.4 m at Changxing section and decreases upward due to friction and river discharge. The M4 tidal amplitude is 0.17 m at Changxing, indicating the significant overtide and tidal asymmetry. The surface 2M2-M4 phase difference is 60º, suggesting a flood tidal asymmetry according to the approach of Friedrichs and Aubrey (1994).

The bottom sediment in SB consists of sands and fine sand with D50 larger than 150-300 μm (Liu et al., 2010). Spatially, they are coarser in the channel and finer over the shallow shoals. This is in line with the usual tide influenced circumstances.

Here we model the decadal morphodynamic development of SB by the process-based Delft3D during the period 1958 and 2007. The aim is to investigate the fluvial channel pattern, the effects of river flow and geometry in controlling fluvial estuarine morphodynamics.

2. Historical evolution of SB

In this study, we call the reaches between Jiangyin and Changxing the South Branch. Now it is a funnel-shaped channel with width increasing from 3 km to 25 km. This geometry is formed due to intensive reclamation along Jiangyin and Xuliujing, reducing the channel width significantly and increasing the channel sinuosity (Yun, 2004). From the map in 1860, the SB was a wide (~13-18 km) and straight channel with large scaled meanders (Fig 2). Later the Liuhai shoal and the Tonghai shoal are successively reclaimed and merged into the bank in 1910s and during 1948-1961, respectively. Thus the upper SB, the reach between Jiangyin and Xuliujing, is narrowed to 3-5 km. At the same time, the deep channel becomes more inflected. The southern coastline of the lower SB is protected well from erosion since 1750s. The northern coastline, also the southern bank of the Chongming Island, is eroded and retreated during 1860 and 1900. Later it is diked successively and become stabilized as well. There are a mid-channel bar, the Baimao shoal, and a bank-attached bar, the Biandan shoal in lower SB. In the downstream end, the mid-channel bar is reclaimed into a fixed island (Changxing Island) during 1960 and 1970. A number of small sands appear ahead the island and locates in the middle of the channel. The evolution of the lower SB is characterized by the development and movement of the bars while its overall morphology has not changes.

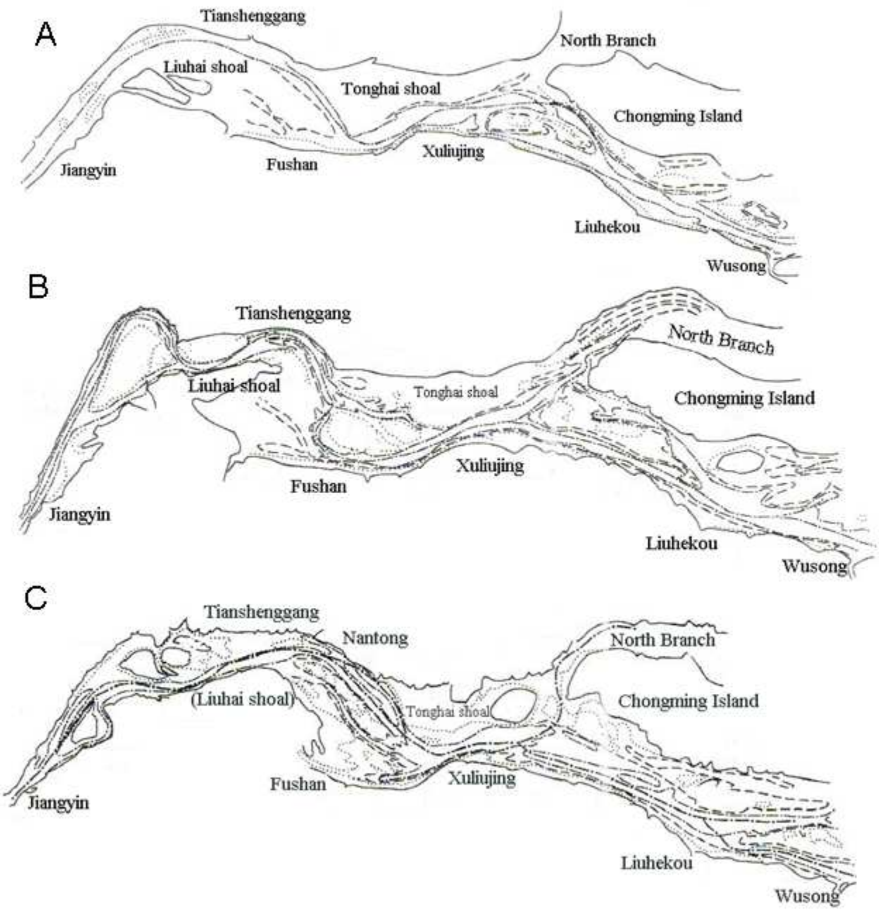

Fig. 2 The sketch map of the outline and the main channel flow in SB (A: 1860; B: 1900-1915; C: 1958. from Yu and Lu (2005))

The channel pattern in SB has taken its shape hundred years ago though the scale of the meanders changes all the time (Fig 2). With matured channel-shoal patterns, the ebb channel gets deepening and is the major passage delivering sediment downward. Secondary flood channels develop such as the one to the north of Biandan shoal and these beside the Changxing Island (Fig 3).

Detailed bathymetry data are available since 1958 in the lower SB. During 1958 and 2007, the lower SB is characterized by rapid accretion of the sands and shoals (Baimao, Zhongyang and Biandan shoals) and deepening of adjacent channels (Fig 3 and 4). This is accompanied by downward movement of the small sands and the lateral shift of the channels (Fig 4).

Hypsometry shows that the deep channel (depth >15 m) experienced erosion between 1958 and 1986 and then the medium depth zone (depth between 5-20 m) during 1986 and 1997 (Fig 5). The bathymetry changes less after 1997 due to fixed coastlines by successive hard engineering works, indicating the approaching toward equilibrium. Overall the channel volume of SB increases by 5% from 1958 to 2007.

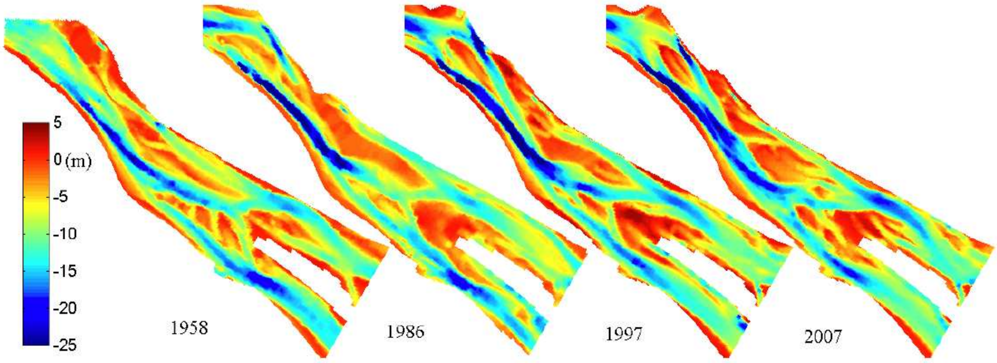

Fig 3 Measured bathymetry (below mean sea level) of lower SB in 1958, 1986, 1997 and 2007

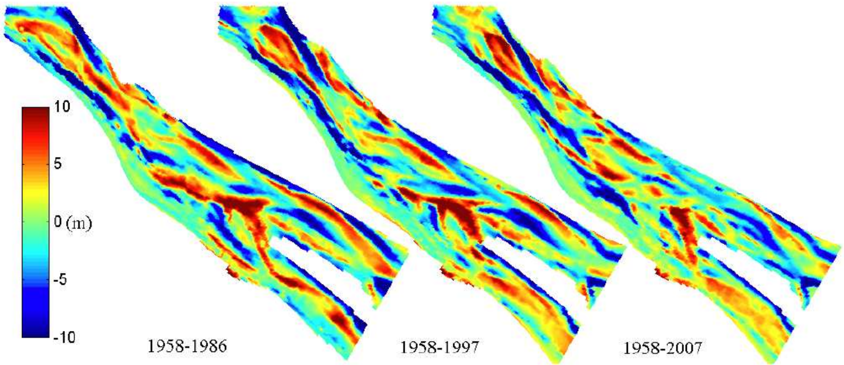

Fig 4 Measured erosion and deposition during 1958 and 2007 in lower SB

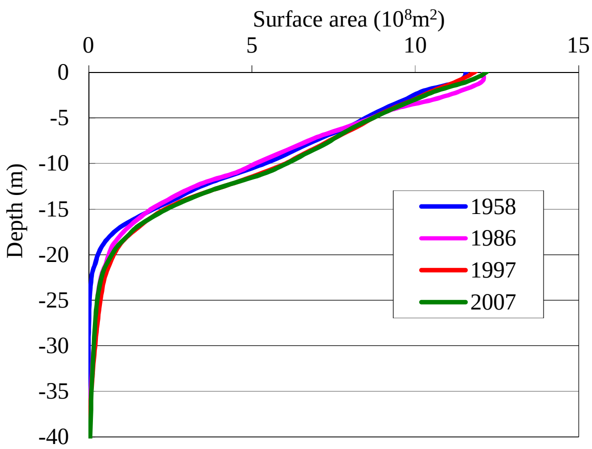

Fig 5 Evolution of hypsometry of lower SB (below MSL)

3. Model setup

In this work we apply the Delft3D morphodynamic model. The Delft3D model system couples hydrodynamic, sediment transport and morphological updating modules systematically. Medium- to long-term morphodynamic modelling is enabled by an online bed level updating scheme and morphological acceleration approach, which is widely used and well validated (Lesser et al., 2004; Roelvink and Renier, 2011; van der Wegen et al., 2008). The details of the hydrodynamic and morphodynamic model techniques in Delft3D are referred to Lesser et al. (2004) and Roelvink and Renier (2011).

The model domain stretches from Datong (DT, the tidal wave limit which is 560 km upstream of Changxing) to Changxing, excluding the NB and the seaward mouth zone (Fig 6). The model is driven by river discharge (seasonal hydrograph) and representative tides (Lesser et al., 2004). The discharge varies from 10,000 m^3/s to 50,000 m^3/s in a year course. The representative tides consists a M2 tide and its first overtide M4 and a virtual C1 tide derived from O1 and K1 tides. The reason and the selection of the representative tides refer to Lesser (2008). One non-cohesive sediment fraction (200 μm) is prescribed with Engelund and Hensen (1967) formula, treating total load transport as bed-load (van der Wegen and Roelvink, 2008). A morphological accelerating factor is deployed to achieve extended morphodynamic evolution results. The sediment boundary conditions are set with equilibrium concentrations and profiles, suggesting unlimited sediment source depending upon the current field. Dry cell erosion and bed slope effect are considered after sensitivity analysis.

After tidal wave calibration, a hydrodynamic model with sediment transport is run to generate an initial bottom composition map. This is achieved by prescribing six sediment fractions, including cohesive and non-cohesive sediments and allowing bed composition changes (van der Wegen et al., 2010). This bed composition model is run based on measured bathymetry in 1958 and no bed level is allowed. Then model would produce a map showing the distribution of D50 of the bottom sediments according to the bathymetry and the current field. This map is used as initial condition in the morphodynamic model with bed level changes.

Hindcasting simulations are carried out for the period 1958-2007. The simulation is done on 2-hydrodynamic-year with a morphological accelerating factor (MF) of 25.

Another simulation with MF 100 is conducted starting from flat bed (mean depth) to see whether and how the model reproduces observed channel patterns. Sensitivity studies are carried out with respect to geometry, presence of overtide and hydrograph variations.

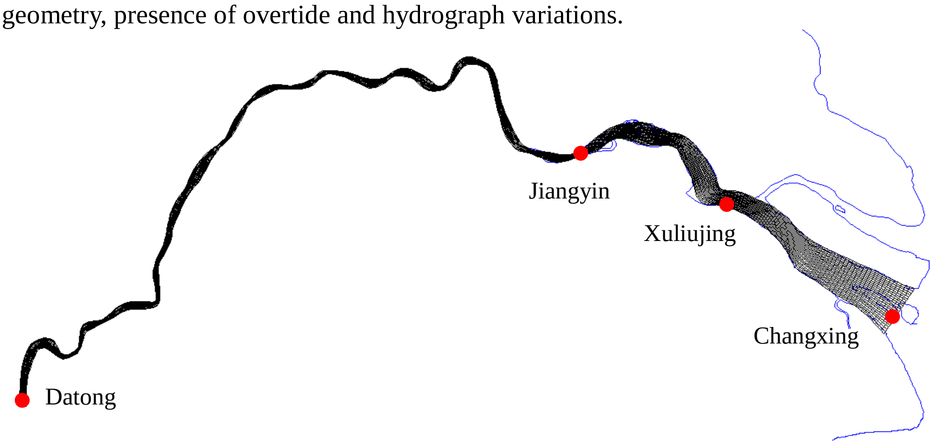

Fig 6 Model domain and grid in YE

4. Result and discussion

4.1 Tidal wave propagation

The tidal wave is damped in the upstream direction though the channel is convergent between Changxing to Jiangyin (Fig 7). It indicates that friction effect and the river discharge play a more significant role in modulating the tide.

The hydrodynamic model simulates the upward damping tidal wave well (Fig 7), suggesting the physical setting in the model is reliable, assuming that the tidal conditions do not change in the past decades. It is also noticed that the large discharge damps the tidal wave much more than small discharge, especially in the upstream reaches, indicating the potential effect of discharge in the driving morphodynamic changes.

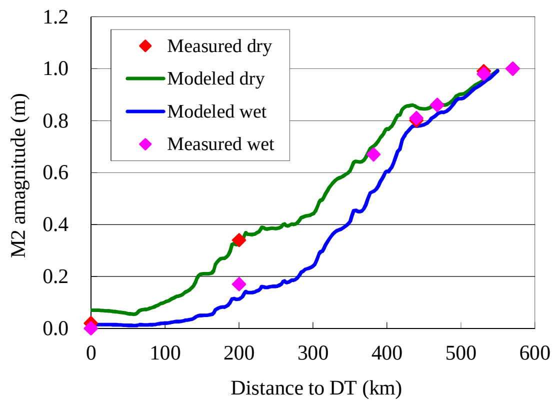

Fig 7 Along-channel M2 tide amplitude variation between Datong and Changxing

4.2 Bottom sediment composition generation

Bottom sediments sampling in SB shows that the bottom sediments are composed of sands with median diameter about 10-300 μm (Liu et al., 2010). Laterally, coarser (150-300 μm) and finer (10-80 μm) materials dominate in the channels and on the flats, respectively. However, field samples do not have high resolution to provide detailed spatial distribution of the bed composition. Thus a bed composition generation scheme is firstly applied as that in van der Wegen et al. (2012) and Dastheigb (2012). The generated bed composition distribution agrees with the measurement fairly in a rough sense, with spatially distributed coarse and fine material between the channels and shoals (Fig 8). Then this bed composition map is used in the morphodynamic model to improve its performance.

Though an initial bed composition map is prescribed in the model, which works better than spatially uniform sediment fraction, it is still noticed that the spatial and temporal bed composition changes associated with channel migration and sands movement are not fully considered in the model. Further simulation with both morphodynamic and bed composition changes is required though it is the computation expensive.

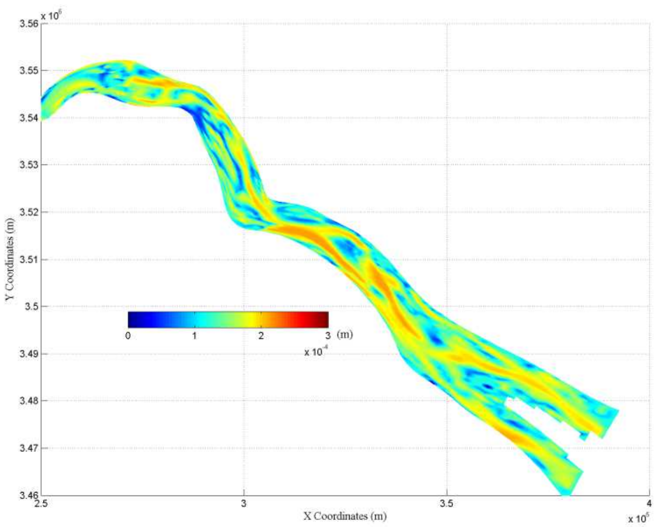

Fig 8 Model generated bed composition in SB based on bathymetry in 1958

4.3 Hindcasting simulation

The modeled bathymetry and erosion and deposition pattern are presented by Figure 9 and 10. In comparing with the measured erosion and deposition map, the overall erosion and deposition magnitude agrees well. In detail, the Baimao shoal is silted up but the extent is underestimated in the model. The channels beside the Baimao shoal deepen as reality. The Biandan shoal and the sands ahead the Changxing Island are also modeled with deposition.

The modeled channel depth is overestimated in the lower segment close to the sea boundary. In reality, the channel depth shallows downward from SB to the mouth zone due to the presence of mouth bars in the turbidity maximum zone. This model discards the mouth zone rudely, thus excluding the sediment exchange between SB and MZ and also the density circulation effect in trapping sediment inside. This simplification could be the reason why the channel develops deeper in this model. However to include the mouth zone in this model domain would lead to more complexity due to the presence of the stratification effect, the wind and wave and also the influence of alongshore coastal currents. It is left for further studies.

In the morphodynamic model, the downward movement of the sands is also simulated (Fig 9). The sand movement is extremely apparent during the large discharge periods, indicating the effect of the fluvial forcing.

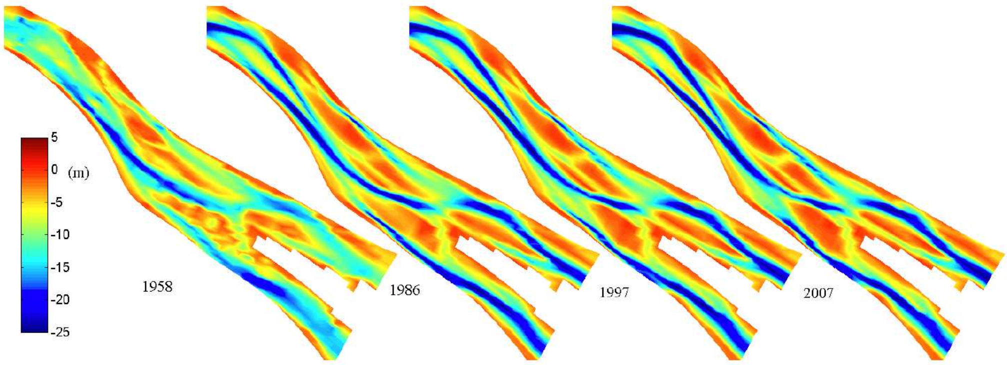

Fig 9 Modeled bathymetries in lower SB in four years

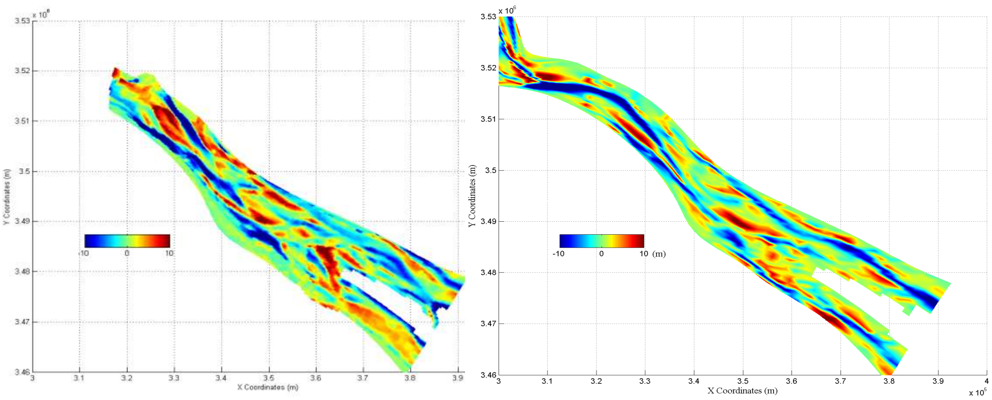

Fig 10 Measured (left) and modeled (right) erosion/deposition of SB from 1958 to 2007

4.4 Channel pattern reproduction

In this simulation, the Changxing Island is excluded in the domain. The schematized model produces a meandering channel-shoal pattern identical with the reality (Fig 11). It is better simulated in the upper SB due to narrowed curved geometry. Discrepancy is observed in the wide lower SB where the channel-shoal pattern is less regular and more divergent. This may be attributed to the large channel width thus more free behavior of the channels and shoals. Moreover, a prescribed uniform bed slope effect in this model could be not perfect for the upper and lower SB at the same time, since the lateral bed slope is much lower in the lower SB (Fig 11).

The wave length of the meanders is proposed to be 6-10 times of the channel width in tide dominated circumstances (Hibma et al., 2004; van der Wegen et al., 2008). Darylmple and Choi (2007) observed that the fluvial dominated channel is more meandered while the tide influenced channel is straighter. Given the SB in YE, both the fluvial and tidal forcings are fundamental. The meander wave length to channel width ratio is relative smaller though the absolute scale of meanders is quite large. This is mainly induced by combined river and tidal forcings and the fixed geometry, whose effect can be seen from the sensitivity analysis.

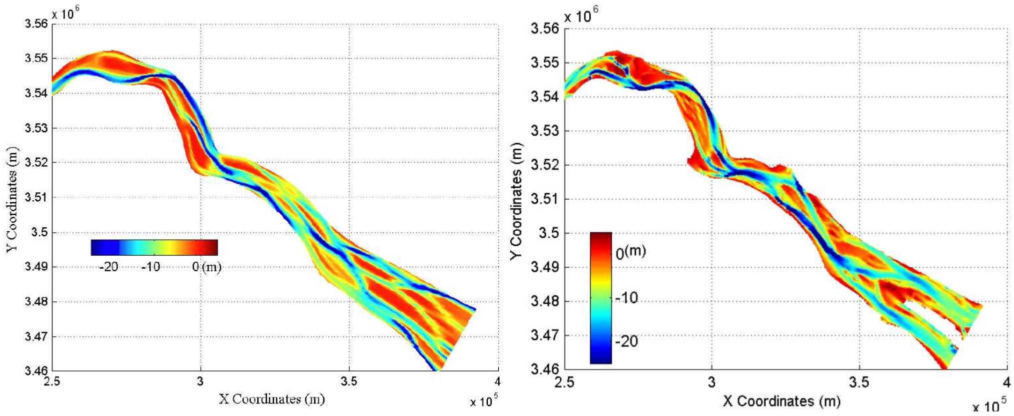

Fig 11 Model reproduced channel pattern (left, after 1000 morphydnamic years) and the measurement in 1997 (right)

4.5 Sensitivity analysis

The sensitivity simulations show us the influence of the geometry, hydrograph and overtide in the morphodynamic evolutions. The case with a flood hydrograph (higher flood peak discharge) shows that the tidal wave is damped more during high discharge, thus relatively enhancing the fluvial influences. Large discharge also leads to higher sediment influx at the river head and sediment deposition in the downstream channels. The reproduced channel-shoal pattern in the lower SB improves in relating the reality though the scales of the channels and shoals are underestimated (Fig 12). However the channel location around Tianshenggang shifts to the north in comparing the normal hydrograph case. This is the result of tidal wave phase changes due to increased river discharge.

The sensitivity case without prescribed overtide has deeper developed channels in the lower section while the channel pattern is more or less the same (Fig 12). It is because the fluvial forcing dominates over the internally generated tidal asymmetry, resulting in more seaward sediment transport.

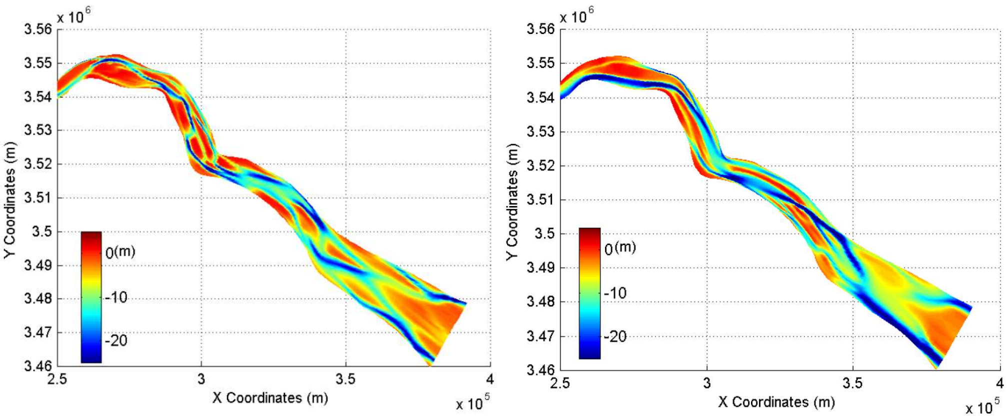

Fig 12 Model produced channel patterns with a flood hydrograph (left) and without prescribed overtide (right)

5. Conclusion

The SB in YE is a fluvial channel with tidal influence. Its morphodynamic evolution during 1958 and 2007 is characterized by shoal accretion and channel deepening, and consequent downward sand movement and channel migration. Since 1997, the morphodynamics in SB develop toward equilibrium with matured channel and shoal pattern, which is presented by dominant meandering ebb channel and secondary flood channel. Overall the channel volume increases by 5% during 1958 and 2007.

To investigate morphodynamic mechanisms in SB, hindcasting simulations are conducted on long-term morphodynamic models. The model produces the deposition over the shallow shoals and erosion along the deep channel within the scaled position, demonstrating the model skill despite its simple setup. Discrepancies between measured and modeled development may be related to the uniform settings such as the roughness and bed slope effect. A prescribed bed sediment composition improves the model performance. The fluvial forcing plays a fundamental role in flushing sediment seaward and driving the downward sand movements.

Starting from a flat bed, the schematized model generates a channel pattern similar with the real pattern. With a prescribed geometry, the meandering channel pattern develops well in the upper SB. It indicates the effect of the geometry in controlling the location of the meanders and channel alignment. The model with flood hydrograph produces well-defined channel pattern in the lower SB due to enhanced fluvial influence. The prescribed overtide generates a flood tidal asymmetry and consequent upward residual sediment transport in the lower channel.

The exclusion of the mouth zone in this model domain leads to poor model performance in the lower SB. The sediment exchange between SB and the mouth zone and the moprhodynamic effect of the mouth bar need further systematical investigation.

Acknowledgement

This study is sponsored by China Scholarship Council (No.2009101208) and ReSeDUE project (No.60038881).

References

Dalrymple, R.W., and Choi, K.S., 2007, Morphologic and facies trends through the fluvial-marine transition in tide-dominated depositional systems: A systematic framework for environmental and sequence-stratigraphic interpretation. Earth Science Reviews, v. 81, p. 135-174.

Dastheigb, A., 2012. Long-term processes-based morphological modeling of large tidal basin. PhD thesis of TUDelft and UNESCO-IHE, Delft.

Engelund, F. and Hansen, E., 1967. A monograph on sediment transport in alluvial streams, Teknisk Forlag, Copenhagen.

Friedrichs, C.T. and D. Aubrey, 1994: Tidal propagation in strongly convergent channels. Journal of Geophysical Research, 99, 3321–3336.

Hibma, A., Stive, M.J.F., Wang, Z.B., 2004. Estuarine morphodynamics. Coastal Engineering, (8-9): 765-778.

Hu, K.L., Ding, P.X., Wang, Z.B. and Yang, S.L., 2009. A 2D/3D hydrodynamic and sediment transport model for the Yangtze Estuary, Chian. Journal of Marine Systems, 77: 114-136 .

Lesser, G.R., Roelvink, J.A., van Kester, J.A.T.M., Stelling, G.S., 2004. Development and validation of a three-dimensional morphological model. Coastal Engineering, 51: 883-915.

Lesser, G.R., 2009. An approach to medium term morphodynamic modeling. PhD thesis of Delft University of Technology, Delft, the Netherlands.

Liu, H., He, Q., Wang, Z.B., Weltje, G.J., Zhang, J., 2010. Dynamics and spatial variability of near-bottom seidment exchange in the Yangtze Estuary, China. Estuarine, Coastal and Shelf Science, 86: 322-330.

Roelvink, J.A. and Reniers, A.J.H.M., 2011. A guide to coastal morphology modeling. (Advances

in Coastal and Ocean Engineering: Volume 12) World Scientific Publishing Company, Singapore.
van der Wegen, M. and Roelvink, J.A., 2012. Reproduction of estuarine bathymetry by means of a process-based model: Western Scheldt case study, the Netherlands, Geomorphology, doi: 10.1016/j.geomorph.2012.08.007.
van der Wegen, M. and Roelvink, J.A., 2008. Long-term morphodynamic evolution of a tidal embayment using a two-dimensional, process-based model. Journal of Geophysical Research, 113,C03016, doi:10.1029/2006JC003983.
van der Wegen, M., Dastgheib, A. and Roelvink, J. A., 2010. Morphodynamic modelling of tidal channel evolution in comparison to empirical PA relationship. Coastal Engineering, 57: 827–837.
van der Wegen, M., Dastgheib, A., Jaffe, B.E. and Roelvink, J.A., 2010. Bed composition generation for morphodynamic modeling: case study of San Pablo Bay in California, USA. Ocean Dyanmics, DOI 10.1007/s10236-010-0314-2.
van der Wegen, M., Wang, Z.B., Savenije, H.H.G. and Roelvink, J.A., 2008. Long-term morphodynamic evolution and energy dissipation in a coastal plain, tidal embayment. Journal of Geophysical Research, 113, F03001, doi:10.1029/2007JF000898.
Wang, Y., Shen, J., and He, Q., 2010. A numerical model study of the transport timescale and change of estuarine circulation due to waterway constructions in the Changjiang Estuary, China. Journal of Marine Systems, 82:154-170.
Wu, H., Zhu, J.R. and Choi, B.H., 2010. Links between salt water intrusion and subtidal circulation in the Changjiang Estuary: a model guide study. Continental Shelf Research., doi:10.1016/j.csr.2010.09.001
Yu, W.C. and Lu, J.Y., 2005. River channel evolution and training in the Yangtze River. Water Resources Press, Beijing, China.
Yun, C.X., 2004. Recent evolution of the Yangtze Estuary and its mechanism. China Ocean Press, Beijing, China.